



Semnan University

# Mechanics of Advanced Composite Structures

journal homepage: <http://MACS.journals.semnan.ac.ir>



## Modeling Aeroelastic Vibration Dampening in Wind Turbine Blades using Piezoelectric Materials

Hadja YAKOUBI<sup>a\*</sup>, Aida CHERIF<sup>b</sup>, Mounir MEDDAD<sup>b</sup>, Issam MEGHLAOU<sup>b</sup>, Nabil DERBEL<sup>c</sup>

<sup>a</sup> LMSE laboratory, Mohammed El Bachir Ellbrahimi University, Bordj Bou Arreridj, Algeria

<sup>b</sup> Electromechanical Department, Mohammed El Bachir Ellbrahimi University, Bordj Bou Arreridj, Algeria

<sup>c</sup> National School of Engineers, Sfax, Tunisia

### KEYWORDS

Wind turbine blades;  
aerodynamic forces;  
SSDI modal;  
Vibration control;  
Piezoelectric materials.

### ABSTRACT

Aeroelastic vibrations, caused by the complex interaction between aerodynamic forces and the structural dynamics of wind turbine blades, are a major contributor to fatigue, structural damage, reduced efficiency, and increased maintenance costs in wind turbine systems. Addressing this issue is critical for enhancing wind turbine's operational performance, durability, and lifespan, making vibration control a key focus in the renewable energy industry. This paper investigates the Synchronized Switch Damping (SSD) modal method, a nonlinear control technique specifically chosen for its ability to efficiently mitigate aeroelastic vibrations by targeting and suppressing unwanted vibration modes. By synchronizing a piezoelectric component with a designated electrical circuit in harmony with the blade's movement, the SSD modal method provides precise and adaptive vibration control. Our study demonstrates the effectiveness of the Semi-active Modal SSD approach, achieving a notable 30.42% reduction in blade vibration. This substantial reduction enhances not only the overall performance but also the longevity of wind turbine blades, offering a significant advancement in vibration control strategies and contributing to the development of more reliable and efficient wind energy systems.

### 1. Introduction

Wind energy has been demonstrated as an important source of clean, environmentally friendly, renewable energy and a green alternative to fossil energy. Thus, there is increasing research in the area of modeling and improving the efficiency of wind turbines, and now it's receiving strong attention from governments and private institutions [1] [2].

The essential components of nearly all wind turbines, whether large or small, are identical: blades, shafts, gears, a generator, and a wire (certain turbines lack gearboxes). These elements collaborate to transform wind energy into electrical power. Generally, the amount of energy that wind turbines can gather depends on the shape of their blades. The blades are made to gather the most wind energy possible and transform it into rotational mechanical energy. Hence, the blades are a massively crucial critical part of a wind turbine [3]. Their operation is

based on the theory of quantity of motion and the theory of blade elements. Several computer codes have been created to evaluate the performance of wind turbines and to define the effects of all aerodynamic parameters such as wind speed, profile type, angle of attack pitch, lift, and drag [4]. Wind turbine blades are increasingly changing in terms of size and complexity, becoming larger and more complex. Their construction includes a wide variety of materials and manufacturing techniques [5]. It is necessary to emphasize the importance of complete analysis and harmonization of all processes in relation to this system, from design (aerodynamic improvement, etc.), regulations and standards, manufacturing, materials and technology, and verification testing. Harmonization of new wind turbine rotor blades development process: [5][6][7][8].

As the blade is subjected to the non-stationary wind force, the vibration problem is becoming

\* Corresponding author. Tel.: +98-99-99999999 ; Fax: +98-99-99999999  
E-mail address: [hadja.yakoubi@univ-bba.dz](mailto:hadja.yakoubi@univ-bba.dz)

increasingly critical as wind turbines grow in size. Vibrations not only cause structural or mechanical damage, but they also reduce the wind turbine's lifetime [9][10]. In recent years, numerous studies have focused on addressing aeroelastic vibrations in wind turbine blades, recognizing the detrimental effects these vibrations can have on performance and longevity [11].

Smart materials are becoming more popular, and evolutions in their area suggested research about their abilities and the use of these materials because they can harvest energy sources in the external environment [12-14]. Piezoelectric materials serve as primary components in energy harvesting, marking the initial phase in converting ambient energy (such as vibration, thermal, solar, etc.) into electrical energy [15-16]. Piezoelectric materials present good performance in controlling vibrations on structures on account of their high integrability, compactness, and slight and high bandwidth ability to operate as actuators or sensors [17]. The piezoelectric effect is classified into two forms: (i) the direct piezoelectric effect states that anytime mechanical strain is exerted on piezoelectric material, it produces electric charges so the piezoelectric element operates as a sensor, and (ii) The inverse piezoelectric effect refers to the capacity of piezoelectric materials to generate strain, functioning as an actuator, in response to an applied electric field [18-19].

Among the types of semi-active and semi-passive vibration damping techniques that use piezoelectric inserts, Richard and Guyomar have created the Synchronized Switch Damping (SSD) approach [20]. SSD methods strike a beneficial balance between user-friendliness, reliance on external energy, and the effectiveness of vibration control. In this non-linear approach, the piezoelectric component is linked periodically to a passive shunt, which consists of a miniature resistance or inductor whenever the voltage (or stress) nears an extreme point [21]. It is achieved using a straightforward switch that is briefly powered in time with the structure's motion. There is no requirement for external operative energy. As a result of the switching process, it is taken from the structure itself. The short-circuit (SSDS) involves activating a low-resistance state in the piezoelectric element, while the short-circuit damping and impedance (SSDI) technique is achieved by incorporating a small inductor into the resistive shunt circuit [22]. The traditional low-powered SSD approaches operate well in mono-modal stimulation, but they struggle with multimodal and complicated vibrations. For the sake of solving the issue of the previous technique, the Modal-SSDI approach has been developed. This approach is particularly suited

for multimodal and complicated vibrations. The switch is coordinated with a particular extreme modal coordinate. It makes use of a modal model of the structure to create a modal observer that allows the modal coordinates describing the structure's motional state to be calculated [23].

While previous research has demonstrated the potential effectiveness of piezoelectric-based damping systems, there remains a need for further synthesis and refinement of existing approaches. By integrating insights from previous studies and leveraging the capabilities of piezoelectric materials, our research aims to pave the way for practical implementation and real-world impact in the field of wind energy.

The outcomes of this study hold significant potential to enhance the performance, reliability, and lifespan of wind turbine blades, thereby contributing to the broader goals of sustainable energy production and environmental stewardship. Through a comprehensive exploration of piezoelectric-based damping techniques, this research seeks to advance state-of-the-art wind turbine technology and accelerate the transition towards a cleaner and more sustainable energy future.

## 2. Aerodynamic Forces Exerted on the Wind Turbine Blades

The most significant force exerted on the blades of a wind turbine is the aerodynamic force caused by the wind. This force is generated by the air flowing over the surface of the blade and is responsible for driving the rotor. The airflow through the rotor of the wind turbine creates pressure deference above and below the blade, which generates the two primary aerodynamic forces exerted upon the blade. The lift force, exerted at a right angle to the wind flow's direction, is accountable for the turbine's output of power, and the resistant drag force, which acts in alignment with the direction of wind flow and opposes the motion of the blade, both of these forces rely on wind velocity, blade velocity and angle of attack [24-25].

$$F_L = \frac{1}{2} \rho S V^2 C_L(\alpha) \quad (1)$$

$$F_D = \frac{1}{2} \rho S V^2 C_D(\alpha) \quad (2)$$

where,  $C_L(\alpha)$  and  $C_D(\alpha)$  represent the lift and drag coefficients, which vary based on the angle of attack  $\alpha$ , and  $\rho$ ,  $V$ , and  $S$  represent, respectively, the air density, the inflow wind velocity, and the area of the blade.

The attack angle, sometimes called the incidence angle, depends on blade twist and pitch.

$$\theta_p + \alpha = \varphi \quad (3)$$

$\theta_p$  The twist refers to the angle formed between the blade's rotation plane and the chord line of the element.

Sometimes,  $\theta_p$  is referred to as the pitch angle.  $\varphi$  presents the inflow angle formed by the inflow wind velocity and the plane of rotation [26-27].

According to the theory of blade element momentum (BEM), we separate the blade into numerous non-reacting radial parts, the lift  $dF_L$  and the drag  $dF$  forces operating on the blade element may be expressed as [20-21]:

$$dF_L = \frac{1}{2} \rho S V_w^2 c_l C_L(\alpha) dr \quad (4)$$

$$dF_D = \frac{1}{2} \rho S V_w^2 c_d C_D(\alpha) dr \quad (5)$$

where  $V_w$  represent the relative wind velocity of the airfoil.  $V_w$  is a resultant vector formed by merging the wind speed approaching the turbine and the rotational speed of the rotor. Furthermore, it is associated with the vibration velocities of the tower and blade, induction factors, lift and drag coefficients, pitch angle, and the twist angle of blade elements at specific cross-sections denoted by  $c_i$ , where  $i$  ranges from 1 to  $N$ .

for the local blade element's crosswise section,  $V_w^2$  can be computed as:

$$V_w^2 = U_i^2 + V^2 \quad (6)$$

$$U_i = \lambda_i V \quad (7)$$

where  $U_i$  represents the rotational velocity of the blade at the specific cross-section  $i$ ,  $V$  and  $\lambda_i$  denote the inflow wind velocity and the tip-speed ratio at that particular cross-section of the blade  $i$ . The value of  $\lambda_i$  can be determined using specific equations:

$$U = \omega R = \lambda V \quad (8)$$

$$U_i = \omega r_i = \lambda_i V \quad (9)$$

$$\lambda_i = \lambda \frac{r_i}{R} \quad (10)$$

where  $U$  is the blade's rotational velocity at its tip,  $\omega$  is the blade's angular velocity,  $\lambda$  is the tip-speed ratio at the blade's tip,  $r_i$  represents the radius of the blade's  $i$ th cross-section, and  $R$  is the blade's radius.

The force ( $F_a$ ) represents the axial constituent of the lift force and the drag force. It's the one that's perpendicular to the rotational plane and bends the blade back against the tower. The axial force denoted as  $dF_a$  exerted on a blade element situated at radius  $r_i$  is indicated by [27] :

$$dF_a = dF_L \cos \varphi_i + dF_D \sin \varphi_i \quad (11)$$

$$F_a = \frac{1}{2} \rho V_w^2 [C_L(\alpha) \cdot \cos(\varphi) + C_D(\alpha) \cdot \sin(\varphi)] \quad (12)$$

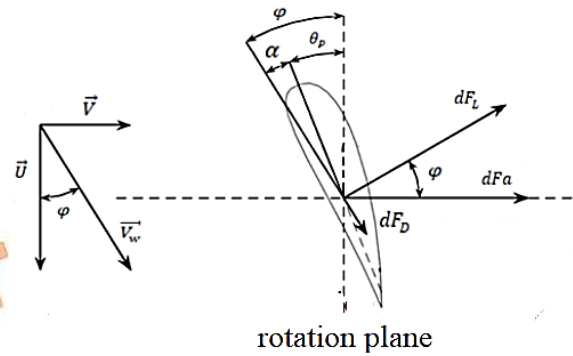


Fig. 1. Velocities and the applied forces on the blade's airfoil[28].

### 3. Method Used

#### 3.1.SSDI Control

The semi-active SSDI (Synchronized Switch Damping on Inductor) method is employed to reduce the undesired vibrations and noise in electronic systems. This technique involves the utilization of piezoelectric materials, which are materials that generate an electrical charge when subjected to mechanical stress, to dampen the vibrations. The implementation of SSDI techniques involves incorporating a switching component alongside the piezoelectric elements. This component is a basic electronic switch connected in parallel, and the switch is in series with a coil of inductance  $LI$  [29-32].

The basic principle behind SSDI is to use a piezoelectric material to generate a voltage directly related to the system's vibration. This voltage is then used to control a switch, which is connected to an inductor. The switch is synchronized with the vibration of the system such that it is closed when the vibration is at a maximum and opened when the vibration is at a minimum. This causes the inductor to generate an opposing current that dampens the vibration. The piezoelectric component is alternately transitioned between an open circuit and a particular electrical threshold, synchronizing with the movement of the structure [30].

The detection of maximum and lowest voltage levels serves as the foundation for the control fundamentals of SSDS and SSDI methods (switching points). Specifically, when an extremum of displacement (or voltage) is sensed in the SSDI circuit, the switch is quickly closed [29-32].

Consequently, the internal capacity of the piezoelectric element ( $C_0$ ) and the inductance ( $L_1$ ) form an oscillating circuit. The oscillating

circuit operates at a resonant frequency that depends on the piezoelectric element's capacitance and the circuit's inductance. The voltage across the piezoelectric component is reversed after the resonant circuit has run for half a time ( $\Delta t_{je}$ ), and the switch is opened again. The time taken for inversion is directly related to the inductance, and the loss of voltage inversion occurs due to losses in the inversion network.

$$t_{ie} = \pi\sqrt{C_0L_1} \quad (13)$$

The voltage inversion defect is caused by inversion network losses; the reversed voltage  $V_{after}$  is less than the voltage preceding the inversion  $V_{prior}$ . An inversion factor is given as follows:

$$V_{after} = -\gamma V_{prior} \quad (14)$$

The  $\gamma$  parameter is connected to the  $(L, C_0)$  oscillating network's electrical quality factor [30].

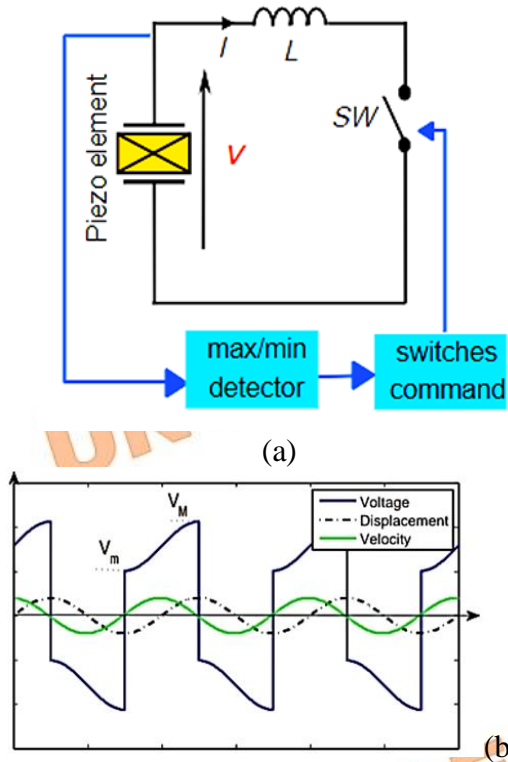


Fig. 2. (a) The SSDI electrical circuit ; (b) SSDI waveforms [33]

### 3.2. Modal SSDI Control

The SSDI modal technique was created because of the disability of the previous control, which was considered broadband stimulation. The suggested method expands the SSD control to accommodate any excitation (not just single mode) and optimizes the damping for specific targeted modes, thus improving the method's effectiveness in reducing vibrations caused by multiple modes [29]. Figure 5 summarizes the

SSDI-Modal strategy, which utilizes modal controllers, with each controller responsible for regulating a single mode. The controllers employ the respective modal coordinates  $q_i$  of the intelligent structure. However, obtaining these modal coordinates requires additional steps as the sensors only measure a voltage that corresponds in proportion to the strain, which cannot directly provide the modal state. The following techniques are employed consecutively: modal observer, SSDI technique, and multimodal control [30]. Its principle is to synchronize the switch sequence on a specific modal coordinate rather than the voltage. The modal displacement extrema can be used to regulate voltage inversion [23].

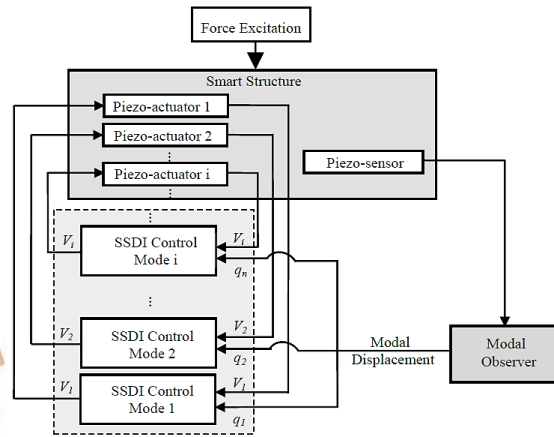


Fig. 3. Principle of Modal-SSDI control [34]

## 4. Smart-Structure Definition :

### 4.1. System Modeling

The purpose of the work described here is to simulate control vibration on wind turbine blades of NACA4412 submitted to a broadband excitation caused by wind force using the program MATLAB/SIMULINK using the fewest actuators and sensors. The method used is the semi-active control SSDI modal developed by Harari [23] based on SSDI control with minimal energy requirements. It applies semi-active control for various types of stimulation while maximizing modal damping on a number of specific modes.

The mechanical and electric equations of a mono-modal smart structure with one piezoelectric element can be written as :

$$m\ddot{\delta} + c\dot{\delta} + k^E\delta = \alpha V + F \quad (15)$$

$$I = -\alpha\dot{\delta} - C_0\dot{V} \quad (16)$$

where  $\delta$  is the displacement of the vibration structure,  $m$ ,  $c$ , and  $k^E$  are, respectively, the mass of the structure, damping coefficient, and

stiffness of the structure of the piezoelectric element is in a short-circuit, and  $\alpha$  is the piezoelectric force coefficient,  $V$  is the piezoelectric element voltage,  $I$  is the electric current, and  $C_0$  is the blocked capacitance of piezoelectric element.  $F$  is the force exerted on the system.

Moreover, in the case of a multi-model structure, the parameters correspond to the  $n$ th modes, which are glued to the  $z$  number of piezoelectric elements.

The previous structure motion  $\delta$  can be modeled as the linear sum of the different modal components. These elements form the modal vector  $q$ , which is connected to  $\delta$  utilizing the structure's mode shape matrix basis  $\phi$ , where  $\phi_j$  is the distorted  $j^{\text{th}}$  mode shape, and  $q_j$  is coordinated with the  $j^{\text{th}}$  mode in the time domain.

$$\delta(x, y, \dots, t) = \sum_{j=1}^n \phi_j(x, y, \dots) \cdot q_j(t) \quad (17)$$

Equations (15) and (16) can be transformed into:

$$m\phi\ddot{q} + c\phi\dot{q} + k^E\phi q = \alpha V + F \quad (18)$$

$$I = -\alpha\phi\dot{q} - C_0\dot{V} \quad (19)$$

By multiplying equation (18) by  $\phi^T$ , it becomes:

$$\phi^T m\phi\ddot{q} + \phi^T c\phi\dot{q} + \phi^T k^E\phi q = \phi^T \alpha V + \phi^T F \quad (20)$$

Equations (20) and (19) can be accurately described using the projection in the modal basis as:

$$M\ddot{q} + C\dot{q} + K^E q = -\theta V + \beta F \quad (21)$$

$$I = \theta^t \dot{q} - C_0 \dot{V} \quad (22)$$

with  $\theta$  the matrix of modal electromechanical coupling with  $[n, i]$  matrix size.  $\theta$  is mentioned below:

$$\theta = \phi^t \alpha \quad (23)$$

$M$ ,  $C$ , and  $K^E$  present the mass, damping, and stiffness modal matrices, respectively, and the mode shape coefficient associated with the position of the excitation force  $F$  is used to construct the  $\beta$  matrix.

Equation (21) is normalized to obtain the identity of the modal mass matrix. As a result, the modal matrices may be represented as functions of the modal damping vector  $\xi$ ,  $\omega^E$  the short-circuit frequency vector, and  $\omega^D$  the open circuit frequency vector as described below:

$$M = I_d; \quad C = 2\text{diag}(\xi)\text{diag}(\omega^D); \quad K^E = ((\omega^E)^2) \quad (24)$$

In the general case, the structure is instrumented by both sensors and actuators. By separating the voltage of the actuators  $V_a$  from that of the sensors  $V_s$ , equation (20) becomes:

$$M\ddot{q} + C\dot{q} + K^E q = -\theta_a V_a - \theta_s V_s + \beta F \quad (25)$$

The sensor intensity registers as zero during an open circuit or when measuring the sensor voltage with a voltage amplifier.

$$\theta_s^t q - C_{0s} V_0 = 0 \quad (26)$$

Furthermore, inserting equation (26) in equation (25) gives:

$$M\ddot{q} + C\dot{q} + (K^E + \theta_s(C_{0s})^{-1}\theta_s^t)q = -\theta_a V_a + \beta F \quad (27)$$

Linear systems (27) and (26) are expressed under the formula in a modal state.

$$\begin{cases} \dot{x} = Ax + Bu \\ y = Cx \end{cases} \quad x = \begin{bmatrix} q \\ \dot{q} \end{bmatrix} \quad (28)$$

$x$  represents the state vector, and  $u=[F, V_a]^T$  is the control vector, which consists of the external mechanical force that the system endured and the actuator voltages applied for damping.

$y = [q, \dot{q}, V_s]^T$  is the output vector, composed of the modal displacements of the structure with its temporal variations and the tensions of the sensors used subsequently by the modal observer, and  $A$ ,  $B$ , and  $C$  represent the state, the control, and the output matrices, respectively:

$$A = \begin{bmatrix} 0 & I_d \\ -M^{-1}(K^E + \theta_s C_{0s}^{-1} \theta_s^t) & -M^{-1}C \end{bmatrix}; \quad B = \begin{bmatrix} 0 \\ +M^{-1}\beta & -M^{-1}\theta_a \end{bmatrix}; \quad C = \begin{pmatrix} I_d & 0 \\ 0 & I_d \\ C_{0s}^{-1}\theta_s^t & 0 \end{pmatrix}; \quad (29)$$

$$V_a \text{ is calculated by the following relation : } V_a = C_{0a}^{-1}\theta_a^t q \quad (30)$$

$C_{0a}$ ,  $C_{0s}$  are respectively the matrix of the actuator's capacity and the matrix of sensors' capacity [23, 29-30].

#### 4.2. Smart-Structure :

In the simulations and evaluations that follow, a wind blade with four P188 piezoelectric insertions will be the structure. Their dimensions and physical characteristics are listed in Tables 1 and 2. Figure 4 depicts this blade. This structure was discovered using the previously outlined

model. Richard's study [35] defines the measuring procedure and parameter identification. Table 2 presents the properties of PZT P189 installs.

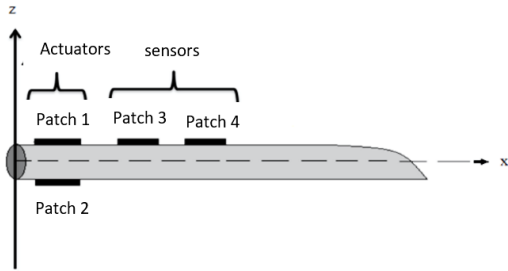


Fig. 4. Integration of piezoelectric elements on the wind turbine blade

Table 1. Blade specification [27].

Airfoil Type	NACA 4412
Total Blades	3
Blades' length	1,5 m
Blades' Base Width	0,15 m
Blades' Tip Width	0,0312 m

Table 2. PZT P189 piezoelectric inserts characteristics [36].

Properties	Symbol	Value
Density	$\rho$	7650 Kg.m <sup>3</sup>
Compliances short-circuit	$S_{11}^E$ $S_{12}^E$	$10.66 \times 10^{-12} Pa^{-1}$

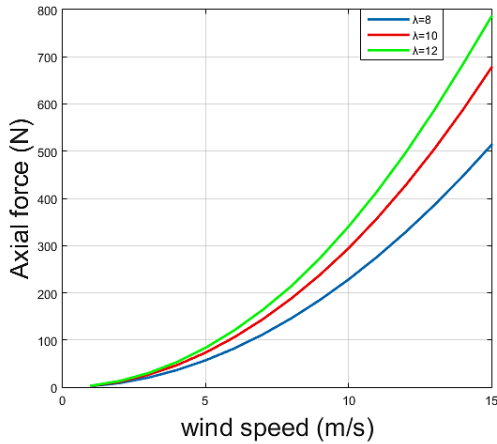


Fig. 5. Wind speed and wind speed ratio  $\lambda$  Effect on axial force on NACA4412

Based on the graph above, there's a positive correlation between the axial force and the wind speed passing through the blade and its rotational speed, which is expressed by the wind speed ratio  $\lambda$ .

The next step is a simulation of the control of the structure's single mode. This single-mode control is analyzed using the following simulation: the random excitation from the variance and mean of the previous axial forces.

	$S_{13}^E$	$-3.34 \times 10^{-12} Pa^{-1}$
	$S_{33}^E$	$-4.52 \times 10^{-12} Pa^{-1}$
		$13.25 \times 10^{-12} Pa^{-1}$
Permittivity	$\epsilon_{33}^T$	$10.17 nF.m^{-1}$
Piezoelectric coefficient	$d_{13}$	$-108 pC.N^{-1}$

## 5. Simulation and Results

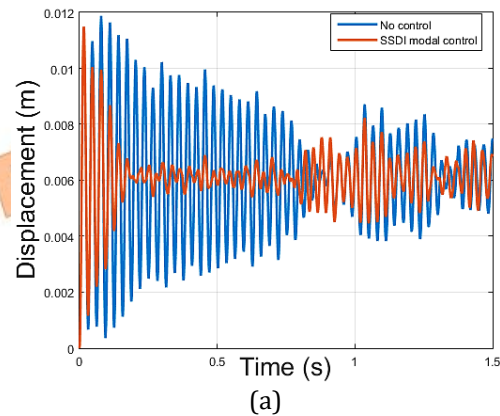
The proposed work mainly consists of numerical simulations of the structure's movement (displacement) and the damping network. Simulations are conducted using the MATLAB/Simulink software environment.

For the first part, a study is being conducted on the behavior of the axial force, as shown in equation (12) of the NACA4412 blade, with respect to changes in wind speed and rotational speed. Axial force refers to the force exerted parallel to the axis of the blade, and NACA4412 is a type of airfoil shape commonly used in aircraft and wind turbine blades.

The study analyzes how wind speed and rotational speed changes affect the axial force exerted on the NACA4412 blade.

Overall, this study aims to provide a better understanding of how the NACA4412 blade responds to changes in wind speed and rotational speed. This could have implications for the design and performance of wind turbines and other systems that utilize this type of blade. The second part of the validation methodology involves controlling the voltage variation of the actuator.

**The excitation random:** signal its variance= $4,7046 \times 10^{-4} N$  and its mean= $239,5663 N$



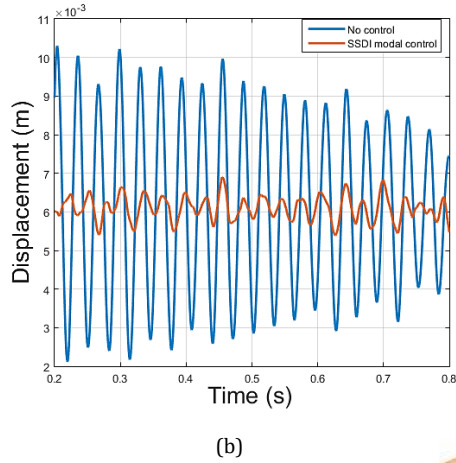


**Fig. 6.** (a) Simulation of the displacement of mode 1 ;(b) zoom in on the interval [0.2s 0.8s]

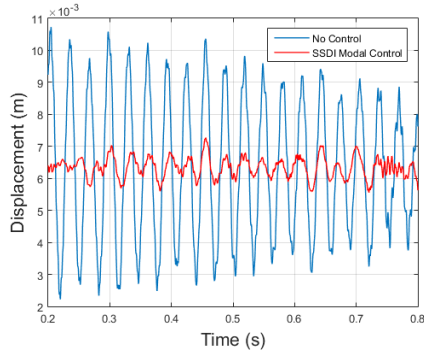


**Fig. 7.** Simulation of the displacement of 3 modes.

**Table 3.** Displacement values before and after applying SSDI modal control of the interval [0.2s 0.8s]

No control	SSDI modal control
$9 \times 10^{-3}$	$6 \times 10^{-3}$
$9.9 \times 10^{-3}$	$6.6 \times 10^{-3}$
$9.4 \times 10^{-3}$	$6.2 \times 10^{-3}$
$9.3 \times 10^{-3}$	$6.3 \times 10^{-3}$
$8.8 \times 10^{-3}$	$6.3 \times 10^{-3}$
$8.5 \times 10^{-3}$	$6.3 \times 10^{-3}$
$7.4 \times 10^{-3}$	$5.5 \times 10^{-3}$

Based on the values in Table 3, the mean percentage reduction in the structure's displacement is 30.42%.

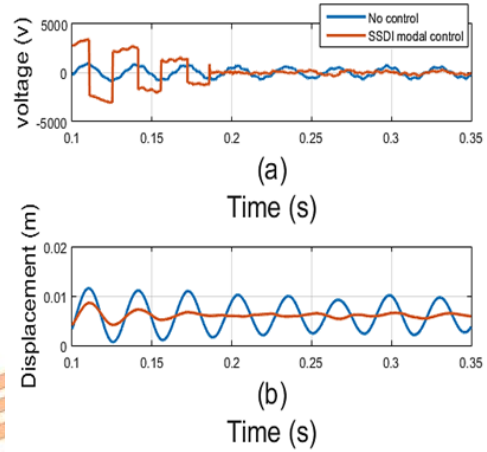


**Fig.8.** (a) voltage of the piezoelectric actuator for a single-mode control ; (b) Modal displacement

The obtained results in Figure 8 and Table 3, compared with the values of vibration of the structure, illustrate the effect of the application of SSDI modal control on the blade's vibration and notice the significant increase in the amplitude voltage at the terminals of the actuator after the control as illustrated in Figure 8a, as well as Figure 8b, explains the results of the voltage growth which is the reason for the increase in actuator performance and therefore improved damping.

## 6. Conclusion

This study delved into the intricate challenge of controlling aeroelastic vibration in wind turbine blades, considering the complex interplay of wind dynamics. Through comprehensive analysis encompassing environmental conditions and design parameters, we aimed to devise a robust control strategy capable of effectively mitigating aeroelastic vibration induced by wind forces.

The results of our investigation underscore the effectiveness of the proposed control technique in minimizing aeroelastic vibration, especially under the influence of stochastic wind excitation. By successfully reducing the impact of wind-induced forces, our approach holds significant practical promise for enhancing both the longevity and performance of wind turbine blades, which is crucial for optimizing wind energy conversion systems.

By leveraging the SSDI semi-active technique and integrating a modal observer, our control strategy not only demonstrates stability and reliability in dynamic wind conditions but also enhances adaptability, enabling effective response to varying wind dynamics across different frequency ranges.

In practical terms, our findings suggest that the developed control strategy offers a promising solution for managing aeroelastic vibration in

wind turbine blades. Thus, it contributes significantly to the advancement of renewable energy technologies and the overall optimization of wind energy systems. This advancement could potentially lead to increased energy production efficiency, reduced maintenance costs, and improved reliability, thereby fostering wider adoption of wind energy as a sustainable power source.

## References

- [1] Erkan, O., Özkan, M., Karakoç, T.H., Garrett, S.J. and Thomas, P.J., 2020. Investigation of aerodynamic performance characteristics of a wind-turbine-blade profile using the finite-volume method. *Renewable Energy*, 161, pp. 1359-1367.
- [2] Yang, W., Kim, K.H. and Lee, J., 2022. Upcycling of decommissioned wind turbine blades through pyrolysis. *Journal of Cleaner Production*, 376, 134292.
- [3] Yang, B. and Sun, D., 2013. Testing, inspecting and monitoring technologies for wind turbine blades: A survey. *Renewable and Sustainable Energy Reviews*, 22, pp. 515-526.
- [4] Debbache, M., 2018. Amélioration de la performance de pale éolienne par considération des paramètres locaux et prend en compte les phénomènes des pertes. Doctoral dissertation, Université Mohamed Khider Biskra.
- [5] Rašuo, B., Dinulović, M., Veg, A., Grbović, A. and Bengin, A., 2014. Harmonization of new wind turbine rotor blades development process: A review. *Renewable and Sustainable Energy Reviews*, 39, pp. 874-882.
- [6] Mirkov, N., Rašuo, B. and Kenjereš, S., 2015. On the improved finite volume procedure for simulation of turbulent flows over real complex terrains. *Journal of Computational Physics*, 287, pp. 18-45.
- [7] Rašuo, B., 2010. Experimental study of structural damping of composite helicopter blades with different cores. *Plastics, Rubber and Composites*, 39(1), pp. 1-5.
- [8] Rašuo, B., 2018. On structural damping of composite aircraft structures.
- [9] Cong, C., 2017. Active control of edgewise vibrations in wind turbine blades using stochastic disturbance accommodating control.
- [10] Gao, R., Yang, J., Yang, H. and Wang, X., 2023. Wind-tunnel experimental study on aeroelastic response of flexible wind turbine blades under different wind conditions. *Renewable Energy*, 219, 119539.
- [11] Biglari, H. and Fakhari, V., 2020. Edgewise vibration reduction of small size wind turbine blades using shunt damping. *Journal of Vibration and Control*, 26(3-4), pp. 186-199.
- [12] Awada, A., Younes, R. and Ilinca, A., 2021. Review of vibration control methods for wind turbines. *Energies*, 14(11), 3058.
- [13] Chakhchaoui, N., Jaouani, H., Ennamiri, H., Eddiai, A., Hajjaji, A., Meddad, M. et al., 2019. Modeling and analysis of the effect of substrate on the flexible piezoelectric films for kinetic energy harvesting from textiles. *Journal of Composite Materials*, 53(24), pp. 3349-3361.
- [14] Farhan, R., Eddiai, A., Meddad, M., Mazroui, M. and Guyomar, D., 2019. Electromechanical losses evaluation by an energy-efficient method using the electrostrictive composites: experiments and modeling. *Smart Materials and Structures*, 28(3), 035024.
- [15] Meddad, M., Eddiai, A., Hajjaji, A., Boughaleb, Y., Guyomar, D. and Fliyou, M., 2014. Optimization of the energy harvested by the effect of strain and frequency on an electrostrictive polymer composite. *Synthetic Metals*, 188, pp. 72-76.
- [16] Meddad, M., Eddiai, A., Guyomar, D., Belkhiat, S., Hajjaji, A., Cherif, A. and Boughaleb, Y., 2012. Study of the behaviour of electrostrictive polymers for energy harvesting with FFT analysis. *Journal of Optoelectronics and Advanced Materials*, 14(1-2), pp. 55-60.
- [17] Harari, S., Richard, C. and Gaudiller, L., 2009. Semi-active control of a targeted mode of smart structures submitted to multimodal excitation. In: *Motion and Vibration Control*, Dordrecht: Springer, pp. 113-122.
- [18] Bahl, S., Nagar, H., Singh, I. and Sehgal, S., 2020. Smart materials types, properties, and applications: A review. *Materials Today: Proceedings*, 28, pp. 1302-1306.
- [19] Rupitsch, S.J., 2019. Simulation of piezoelectric sensor and actuator devices. In: *Piezoelectric Sensors and Actuators. Topics in Mining, Metallurgy and Materials Engineering*, pp. 83-126.
- [20] Chérif, A., Richard, C., Guyomar, D., Belkhiat, S., Meddad, M., Eddiai, A. and Hajjaji, A., 2013. Modal SSDI-Max technique of a smart beam structure: Broadband excitation. *Journal of*



- Optoelectronics and Advanced Materials, 15(May-June), pp. 438-446.
- [21] Chérif, A., Attoui, H., Zehar, D. and Behih, K., 2017. Improved vibration control of a smart beam by energy transfer. *International Journal of Latest Trends in Engineering and Technology*, 8(4), pp. 86-93.
- [22] Asanuma, H. and Komatsuzaki, T., 2020. Nonlinear piezoelectricity and damping in partially-covered piezoelectric cantilever with self-sensing synchronized switch damping on inductor circuit. *Mechanical Systems and Signal Processing*, 144, 106867.
- [23] Wu, D., 2013. Piezoelectric semi-active networks for structural vibration damping with energy redistribution. Doctoral dissertation, Lyon, INSA.
- [24] Schubel, P.J. and Crossley, R.J., 2012. Wind turbine blade design. *Energies*, 5(9), pp. 3425-3449.
- [25] El Mouhsine, S., Oukassou, K., Ichenial, M.M., Kharbouch, B. and Hajraoui, A., 2018. Aerodynamics and structural analysis of wind turbine blade. *Procedia Manufacturing*, 22, pp. 747-756.
- [26] Wood, D., 2011. Small wind turbines. In: *Advances in Wind Energy Conversion Technology*. Berlin, Heidelberg: Springer, pp. 195-211.
- [27] Wang, Y., Liang, M. and Xiang, J., 2014. Damage detection method for wind turbine blades based on dynamics analysis and mode shape difference curvature information. *Mechanical Systems and Signal Processing*, 48(1-2), pp. 351-367.
- [28] Optimisation et régulation des puissances d'une éolienne à base d'une MADA, 2009. Mémoire de magister, École Nationale Supérieure Polytechnique d'Alger.
- [29] Chérif, A., Richard, C., Guyomar, D., Belkhiat, S. and Meddad, M., 2012. Simulation of multimodal vibration damping of a plate structure using a modal SSDI-Max technique. *Journal of Intelligent Material Systems and Structures*, 23(6), pp. 675-689.
- [30] Harari, S., Richard, C. and Gaudiller, L., 2009. New semi-active multi-modal vibration control using piezoceramic components. *Journal of Intelligent Material Systems and Structures*, 20(13), pp. 1603-1613.
- [31] Meddad, M., Eddiai, A., Cherif, A., Guyomar, D. and Hajjaji, A., 2016. Enhancement of electrostrictive polymer power harvesting using new technique SSHI-Max. *Optical and Quantum Electronics*, 48(2), pp. 1-10.
- [32] Silva, T., Tan, D., De Marqui, C. and Erturk, A., 2019. Vibration attenuation in a nonlinear flexible structure via nonlinear switching circuits and energy harvesting implications. *Journal of Intelligent Material Systems and Structures*, 30(7), pp. 965-976.
- [33] Li, K., 2011. Amortissement vibratoire avec échange d'énergie synchronisé entre des éléments piézoélectriques. Doctoral dissertation, INSA de Lyon.
- [34] Harari, S., 2009. Contrôle modal semi-actif et actif à faible consommation énergétique par composants piézoélectriques. Doctoral dissertation, INSA de Lyon.
- [35] Richard, T., 2007. Diminution du coefficient de transmission acoustique d'une paroi à l'aide d'amortisseurs piézoélectriques semi-passifs. Doctoral dissertation, INSA de Lyon.